The antiparasitic agent ivermectin induces chloride-dependent membrane hyperpolarization and cell death in leukemia cells

*Sumaiya Sharmeen,[1] *Marko Skrtic,[1] *Mahadeo A. Sukhai,[1] Rose Hurren,[1] Marcela Gronda,[1] Xiaoming Wang,[1] Sonali B. Fonseca,[2] Hong Sun,[1] Tabitha E. Wood,[1,3] Richard Ward,[1] Mark D. Minden,[1] Robert A. Batey,[3] Alessandro Datti,[4,5] Jeff Wrana,[4] Shana O. Kelley,[2] and Aaron D. Schimmer[1]

[1]Princess Margaret Hospital, Ontario Cancer Institute, Toronto, ON; [2]Department of Pharmaceutical Sciences, Faculty of Pharmacy, University of Toronto, Toronto, ON; [3]Department of Chemistry, University of Toronto, Toronto, ON; [4]Samuel Lunenfeld Research Institute, Mount Sinai Hospital, Toronto, ON; and [5]Department of Experimental Medicine and Biochemical Sciences, University of Perugia, Perugia, Italy

To identify known drugs with previously unrecognized anticancer activity, we compiled and screened a library of such compounds to identify agents cytotoxic to leukemia cells. From these screens, we identified ivermectin, a derivative of avermectin B1 that is licensed for the treatment of the parasitic infections, strongyloidiasis and onchocerciasis, but is also effective against other worm infestations. As a potential antileukemic agent, ivermectin induced cell death at low micromolar concentrations in acute myeloid leukemia cell lines and primary patient samples preferentially over normal hematopoietic cells. Ivermectin also delayed tumor growth in 3 independent mouse models of leukemia at concentrations that appear pharmacologically achievable. As an antiparasitic, ivermectin binds and activates chloride ion channels in nematodes, so we tested the effects of ivermectin on chloride flux in leukemia cells. Ivermectin increased intracellular chloride ion concentrations and cell size in leukemia cells. Chloride influx was accompanied by plasma membrane hyperpolarization, but did not change mitochondrial membrane potential. Ivermectin also increased reactive oxygen species generation that was functionally important for ivermectin-induced cell death. Finally, ivermectin synergized with cytarabine and daunorubicin that also increase reactive oxygen species production. Thus, given its known toxicology and pharmacology, ivermectin could be rapidly advanced into clinical trial for leukemia. (*Blood*. 2010;116(18): 3593-3603)

Introduction

Antimicrobials with previously unrecognized anticancer activity can be rapidly repositioned for this new indication given their extensive prior pharmacology and toxicology testing. For example, the broad spectrum antiviral ribavirin was found to suppress oncogenic transformation by disrupting the function and subcellular localization of the eukaryotic translation initiation factor eIF4E.[1,2] As such, ribavirin was recently evaluated in a phase I dose escalation study in patients with relapsed or refractory M4/M5 acute myeloid leukemia (AML). In this study of 13 patients treated with ribavirin, there was 1 complete remission and 2 partial remissions. Thus, ribavirin may be efficacious for the treatment of AML.[3] Likewise, the antifungal agent ketoconazole inhibits the production of androgens from the testes and adrenals in rats. Given this finding, ketoconazole was rapidly advanced into clinical trials for patients with prostate cancer where it displayed clinical efficacy in early studies.[4,5]

Recently, we demonstrated that the antiparasitic agent clioquinol inhibits the proteosome and induces cell death in leukemia and myeloma cells through copper-dependent and -independent mechanisms.[6] Thus, our preclinical data suggest that this antiparasitic could be repurposed for the treatment of hematologic malignancies. Therefore, we initiated a phase 1 study to evaluate the dose-limiting toxicity, maximum tolerated dose, and recommended phase 2 dose of clioquinol in patients with relapsed or refractory hematologic malignancies (ClinicalTrials.gov ID NCT00963495).

Here, we used a chemical screen to identify known drugs with previously unrecognized activity against leukemia. From this screen, we identified the antiparasitic agent, ivermectin. Ivermectin is a derivative of avermectin B1 and licensed for the treatment of the parasitic infections, strongyloidiasis and onchocerciasis, as well as other worm infestations (eg, ascariasis, trichuriasis, and enterobiasis), but has not been previously tested as an anticancer agent. As part of the development of this agent as an antiparasitic agent, ivermectin was extensively evaluated for its pharmacology, safety, and toxicity in humans and animals. For example, the LD_{50} of oral ivermectin in mice, rats, and rabbits ranges from 10 to 50 mg/kg.[7] In humans, when used to treat onchocerciasis, 100-200 μg/kg ivermectin is administered as a single dose.[8] This brief and low-dose treatment is sufficient to achieve an antiparasitic effect, but higher doses and treatment beyond 1 day have been safely administered for other conditions. For example, in patients with spinal injury and resultant muscle spasticity, up to 1.6 mg/kg ivermectin was administered subcutaneously twice weekly for up to 12 weeks. In this study, no significant adverse effects were reported.[9] Likewise, to evaluate the safety of oral ivermectin, healthy volunteers received 30-120 mg on days 1, 4, and 7 and then a further dose in week 3.[10] Even at a dose of 120 mg (~2 mg/kg),

Submitted January 5, 2010; accepted July 11, 2010. Prepublished online as *Blood* First Edition paper, July 19, 2010; DOI 10.1182/blood-2010-01-262675.

*S.S., M.S., and M.A.S. contributed equally to this work.

The online version of this article contains a data supplement.

The publication costs of this article were defrayed in part by page charge payment. Therefore, and solely to indicate this fact, this article is hereby marked "advertisement" in accordance with 18 USC section 1734.

no serious adverse effects were noted. Finally, reports of ivermectin overdoses also support the evaluation of high doses of ivermectin in humans, as in the majority of these cases no serious adverse events were reported.[11]

In our current study, we demonstrated that ivermectin displayed preclinical activity against hematologic malignancies in vitro and delayed tumor growth in vivo at concentrations that appear pharmacologically achievable. Mechanistically, ivermectin induced chloride influx, membrane hyperpolarization, and generated reactive oxygen species (ROS). Furthermore, ivermectin synergized with cytarabine and daunorubicin. Thus, given its prior safety and toxicity testing, ivermectin could be rapidly advanced into clinical trial for patients with leukemia.

Methods

Reagents

The compounds in the chemical library were purchased from Sigma-Aldrich. Annexin V–fluorescein isothiocyanate (FITC) and propidium iodide (PI) were purchased from Biovision. Indo-1 AM, 6-methoxy-N-(3-sulfopropyl) quinolinium (SPQ), carboxydichlorofluorescein diacetate (Carboxy H_2DCF-DA), 5,5′,6,6′-tetrachloro-1,1′,3,3′-tetraethyl benzimidazlycarbocyanine iodide (JC1), and bis-(1,3-dibutylbarbituric acid)trimethine oxonol ($DiBAC_4(3)$) were all purchased from Invitrogen Canada.

Cell lines

Human leukemia (OCI-AML2, HL60, U937, KG1a) and prostate cancer (DU145 and PPC-1) cell lines and murine leukemia (MDAY-D2) cells were maintained in RPMI 1640 medium. Medium was supplemented with 10% fetal bovine serum (FBS), 100 μg/mL penicillin, and 100 U/mL streptomycin (all from Hyclone). TEX human leukemia cells were maintained in Iscove modified Dulbecco medium (IMDM), 15% FBS, 1%, penicillin-streptomycin, 20 ng/mL SCF, and 2 ng/mL IL-3. All cells were incubated at 37°C in a humidified air atmosphere supplemented with 5% CO_2.

Primary cells

Primary human AML samples were isolated from fresh bone marrow and peripheral blood samples of consenting patients and mononuclear cells fractionated by Ficoll separation. Similarly, primary normal hematopoietic mononuclear cells were obtained from healthy consenting volunteers donating peripheral blood stem cells (PBSCs) for stem cell transplantation. Primary cells were cultured at 37°C in IMDM, supplemented with 20% FBS, and appropriate antibiotics. The collection and use of human tissue for this study were approved by the University Health Network institutional review board.

Chemical screen for cytotoxic compounds

HL60, KG1a, and OCI-AML2 leukemia cells were seeded into 96-well polystyrene tissue culture plates (Nunc). After seeding, cells were treated with aliquots of the chemical library (n = 100) at increasing concentrations (3-50μM), with a final dimethyl sulfoxide (DMSO) concentration of 0.5%. Seventy-two hours after incubation, cell proliferation and viability were measured by the MTS assay. Liquid handling was performed by a Biomek FX Laboratory Automated Workstation (Beckman Coulter).

Cell viability assays

Cell growth, viability, and clonogenic growth of primary cells were measured as described in the supplemental Methods (available on the *Blood* Web site; see the Supplemental Materials link at the top of the online article).

Assessment of ivermectin's anticancer activity in mouse models of leukemia

MDAY-D2 murine leukemia cells, K562, and OCI-AML2 human leukemia cells (2.5×10^5) were injected subcutaneously into the flanks of sublethally irradiated (3.5 Gy) nonobese diabetic/severe combined immunodeficiency (NOD/SCID) mice (Ontario Cancer Institute, Toronto, ON). Four (OCI-AML2), 5 (MDAY-D2), or 7 (K562) days after injection, once tumors were palpable, mice were then treated daily for 10 days (K562) or treated with 8 doses over 10 days (OCI-AML2) with ivermectin (3 mg/kg) by oral gavage in water or vehicle control (n = 10 per group). MDAY-D2 mice were treated similarly, but dosage escalated from 3 (4 days) to 5 (3 days) and 6 mg/kg (3 days) as the drug was well tolerated. Tumor volume (tumor length × width^2 × 0.5236) was measured 3× a week using calipers. Fourteen (MDAY-D2), 15 (OCI-AML2), or 17 (K562) days after injection of cells, mice were killed, tumors were excised, and the volume and mass of the tumors were measured.

To measure gene expression changes in vivo, OCI-AML2 cells (2.5×10^5) were injected subcutaneously into the flanks of sublethally irradiated NOD/SCID mice. Once tumors were established, mice were treated with ivermectin (7 mg/kg) or vehicle control intraperitoneally for 5 days. After treatment, mice were killed and tumors were harvested. mRNA was extracted and changes in STAT expression were measured by quantitative reverse-transcription polymerase chain reaction (qRT-PCR). Evidence of apoptosis was measured by Tunel staining and immunohistochemistry (Pathology Research Program, University Health Network, Toronto, ON).

All animal studies were carried out according to the regulations of the Canadian Council on Animal Care and with the approval of the Ontario Cancer Institute Animal Ethics Review Board.

Intracellular ion measurements

Intracellular chloride concentration was measured using a fluorescent indicator for chloride, SPQ as previously described.[12] Upon binding halide ions such as chloride, SPQ is quenched, resulting in a decrease in fluorescence without a shift in wavelength. After treating OCI-AML2 (5×10^5) and DU145 (4×10^5) cells overnight with ivermectin (3-10μM), cells were incubated for 15 minutes with SPQ (5mM) at 37°C in a hypotonic solution of Hanks balanced salt solution (HBSS/H_2O; 1:1) to promote the intracellular uptake of SPQ. After 15 minutes of incubation with SPQ, cells were diluted (15:1) in HBSS and centrifuged. The supernatant was removed, and cells were resuspended in 200 μL of fresh HBSS and incubated for 15 minutes at 37°C to allow recovery from the hypotonic shock. Cells were then stained with PI, and SPQ fluorescence was determined in the PI negative cells using an LSR-II flow cytometer (Becton Dickinson; excitation 351 nm, emission 485 nm). In parallel, changes in cell size were determined by measuring forward light scatter by flow cytometry. Results were analyzed with FlowJo, version 8.8 (TreeStar).

Changes in cytosolic calcium concentration were detected with the fluorescent dye, Indo-1 AM (final concentration 6μM) as previously described.[13]

Determination of plasma and mitochondrial membrane potential and ROS generation

Plasma and mitochondrial membrane potential were measured by staining cells with $DiBAC_4(3)$ and JC-1 (Invitrogen), respectively, as described above. Intracellular ROS were detected by staining cells with Carboxy-H_2DCFDA (final concentration 10μM) and analyzing with flow cytometry as previously described[14] and as described in the supplemental Methods.

Gene expression studies

OCI-AML2 leukemia cells were treated with buffer control or ivermectin (3μM) for 30 and 40 hours. After treatment, cells were harvested, total RNA was isolated, and gene expression was measured as described in the supplemental Methods.

Drug combination studies

The combination index (CI) was used to evaluate the interaction between ivermectin and cytarabine or daunorubicin as previously described.[15] OCI-AML2 and U937 cells were treated with increasing concentrations of

ivermectin, cytarabine, and daunorubicin. Seventy-two hours after incubation, cell viability was measured by the MTS [3-(4,5 dimethylthiazol-2-yl)-5-(3-carboxymethoxyphenyl)-2-(4-sulfophenyl)-2H-tetrazolium] assay. The CalcuSyn median effect model was used to calculate the CI values and evaluate whether the combination of ivermectin with cytarabine or daunorubicin was synergistic, antagonistic, or additive. CI values of < 1 indicate synergism, CI $= 1$ indicate additivity, and CI > 1 indicate antagonism.[16]

Results

A chemical screen identifies ivermectin with potential anticancer activity

Off- and on-patent drugs with previously unrecognized anticancer activity can be rapidly repurposed for this new indication given their prior toxicology and pharmacology testing. To identify such compounds, we compiled a small chemical library (n = 100) focused on antimicrobials and metabolic regulators with wide therapeutic windows and well-understood pharmacokinetics. We treated OCI-AML2, HL60, and KG1a leukemia cell lines with aliquots of this chemical library at 5 concentrations (ranging from 3-50μM). Seventy-two hours after incubation, cell growth, and viability were measured by the MTS assay. From this screen, we identified ivermectin that reduced cell viability in all cell lines in the screen with an $EC_{50} < 10\mu M$. The results for the screen of OCI-AML2 cells with compounds added at a final concentration of 6μM are shown in Figure 1A.

Ivermectin is cytotoxic to malignant cell lines and primary patient samples

Having identified ivermectin in our chemical screens, we tested the effects of ivermectin on cell growth and viability in a panel of 5 leukemia cell lines. Cells were treated with increasing concentrations of ivermectin, and 72 hours after incubation, cell growth and viability were assessed by the MTS assay. Ivermectin decreased the viability of the tested leukemia cell lines with an EC_{50} of approximately 5μM (Figure 1B). The loss of viability was detected at 24 hours after treatment and increased in a time-dependent manner. Cell death and apoptosis were confirmed by annexin V and PI staining (Figure 1C). Cell death was caspase-dependent, as cotreatment with the pan-caspase inhibitor z-VAD-fmk abrogated cell death (supplementary Figure 1A). Furthermore, times and concentrations of ivermectin that preceded cell death induced G_2 cell-cycle arrest (supplemental Figure 1B and data not shown).

Given the cytotoxicity of ivermectin toward leukemia cell lines, we compared its cytotoxicity to primary normal hematopoietic cells and AML patient samples (n = 4 intermediate risk cytogenetics, n = 1 good risk cytogenetics, and n = 1 unknown cytogenetics). Normal hematopoietic cells and patient sample cells were treated for 48 hours with increasing concentrations of ivermectin. After incubation, cell viability was measured by annexin V and PI staining. Ivermectin was cytotoxic to AML patient samples at low micromolar concentrations. In contrast, it did not induce cell death in the PBSCs at concentrations up to 20μM (Figure 1C). However, when gating on the $CD34^+$ cells from one PBSC sample, ivermectin induced cell death with an IC_{50} of $10.5 \pm 0.6\mu M$. Thus, ivermectin induced cell death in primary AML cells preferentially over normal cells, but the therapeutic window over normal stem cells may be narrow.

Ivermectin was also evaluated in clonogenic assays in primary normal hematopoietic and AML cells. Ivermectin (6μM) had minimal effects on the clonogenic growth of normal hematopoietic cells (n = 3) with $< 15\%$ reduction in clonogenic growth. In contrast, ivermectin reduced clonogenic growth by $\geq 40\%$ in 3 of 6 primary AML samples (Figure 1D). Similar effects were noted when primary cells were directly plated into clonogenic assays with ivermectin (supplemental Figure 2).

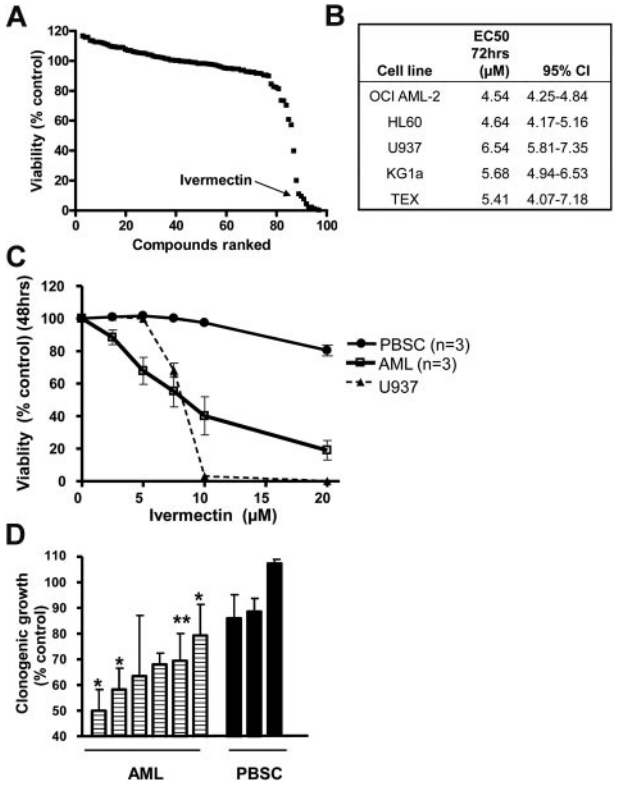

Figure 1. A screen of off-patent drugs identifies the antiparasitic agent, ivermectin, that reduces viability of leukemia cells. (A) OCI-AML2 cells were treated with aliquots of a small chemical library (n = 100) focused on antimicrobials and metabolic regulators. Seventy-two hours after incubation, cell growth and viability were measured by the MTS assay. Data represent the percentage of viable OCI-AML2 cells treated with the compounds (6μM) sorted in order of increasing activity. (B) Leukemia cell lines were treated with increasing concentrations of ivermectin. Seventy-two hours after incubation, cell growth and viability were measured by the MTS assay. Data represent the mean EC_{50} and 95% CI from 3 independent experiments. (C) Primary normal hematopoietic cells (PBSC; n = 3), primary AML patient samples (AML; n = 3), and U937 leukemia cells were treated with increasing concentrations of ivermectin for 48 hours. After incubation, cell viability was measured by annexin V and PI staining. Data represent the mean ± SD percent viable cells from experiments performed in triplicate. (D) Primary AML cell samples (AML; n = 6) and normal hematopoietic peripheral blood stem cell samples (PBSC; n = 3) were treated with ivermectin (6μM) for 24 hours and then plated in a methylcellulose colony forming assay. Seven (AML) or 14 days (PBSCs) days after plating, the number of colonies was counted. Data represent the mean ± SD percent colony formation compared with control treated cells.

Ivermectin delays tumor growth in mouse models of leukemia

Given the effects of ivermectin as a potential antileukemic agent, we evaluated ivermectin in mouse models of leukemia. Human leukemia (OCI-AML2 and K562) and murine leukemia (MDAY-D2) cells were injected subcutaneously into the flank of NOD/SCID mice. Four (OCI-AML2), 5 (MDAY-D2), or 7 (K562) days after injection, once tumors were palpable, mice were treated with ivermectin (3 mg/kg) by oral gavage in water or vehicle control (n = 10 per group) for 10 days (K562) or 8 doses over 10 days (OCI-AML2). MDAY-D2 mice (n = 10 per group) were treated similarly, but with escalating doses (3 mg/kg for 4 days, 5 mg/kg

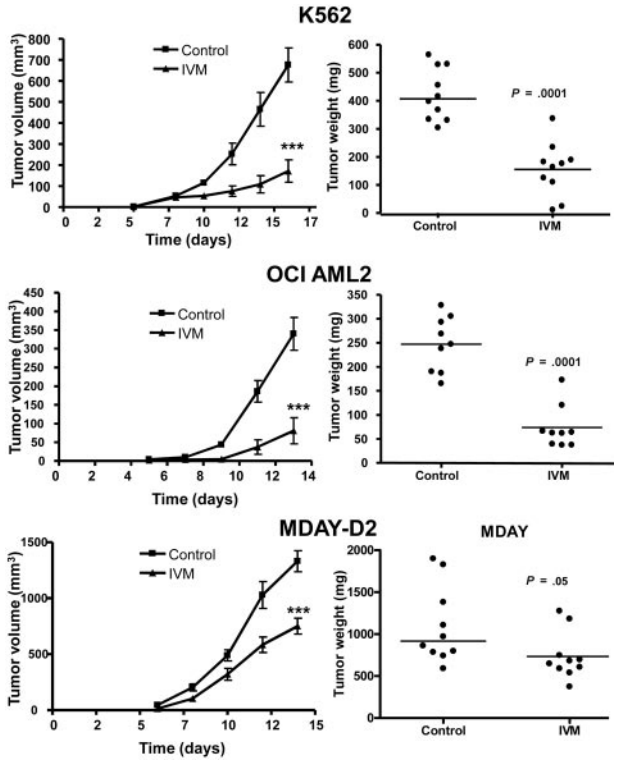

Figure 2. Ivermectin delays tumor growth and reduces tumor mass in leukemia mouse xenografts. Human leukemia (OCI-AML2 and K562) and murine leukemia (MDAY-D2) cells were injected subcutaneously into the flank of sublethally irradiated NOD/SCID mice. Four (OCI-AML2), 5 (MDAY-D2), or 7 (K562) days after injection, once tumors were palpable, mice were treated with ivermectin (IVM; 3 mg/kg) by oral gavage in water or vehicle control (n = 10 per group) for 10 days (K562) or 8 doses over 10 days (OCI-AML2). MDAY-D2 mice (n = 10 per group) were treated with escalating doses of ivermectin (3 mg/kg for 4 days, 5 mg/kg for 3 days, and then 6 mg/kg for 3 days). Fourteen (OCI-AML2), 15 (MDAY-D2), or 17 (K562) days after injection of cells, mice were killed, tumors were excised, and the volume and mass of the tumors were measured. The tumor weight and the mean volume ± SEM are shown. Differences in tumor volume and weight were analyzed by an unpaired *t* test. ***$P < .0001$.

for 3 days, and then 6 mg/kg for 3 days) as the drug was well tolerated. Tumor volume and mass were measured over time. Compared with buffer control, oral ivermectin significantly ($P < .05$) decreased tumor mass and volume in all 3 models (Figure 2) by up to 70% without any gross organ toxicity. In an OCI-AML2 xenograft, we showed that ivermectin increased apoptosis in the subcutaneous tumor as measured by Tunel staining (supplemental Figure 3). Of note, a dose of 3 mg/kg in mice translates to a dose of 0.24 mg/kg in humans, based on scaling of body weight and surface area, and appears readily achievable based on prior studies.[9,11] Thus, the activity in the xenograft studies and the in vitro studies above suggests that a therapeutic window may be achievable.

Ivermectin induces intracellular chloride flux, increase in cell size, and hyperpolarization of the plasma membrane

As an antiparasitic agent, ivermectin activates chloride channels in nematodes, causing an influx of chloride ions into the nematode's cells.[17] Thus, we investigated chloride flux after ivermectin treatment in OCI-AML2 leukemia cells where ivermectin induced cell death after 24 hours of treatment and DU145 prostate cancer cells that were more resistant to ivermectin-induced cell death (Figure 3A). OCI-AML2 and DU145 cells were treated with 10μM ivermectin for 2 hours, and levels of intracellular chloride were measured by staining cells with the fluorescent dye SPQ that is quenched at high chloride ion concentrations. In OCI-AML 2 cells, ivermectin decreased SPQ fluorescence, consistent with an increase in levels of intracellular chloride at concentrations that induced cell death, but at times that preceded cell death (Figure 3B and data not shown). In contrast, chloride influx was not observed in DU145 cells that were resistant to 10μM ivermectin (Figure 3C and data not shown).

Chloride influx can increase cell size. Therefore, we measured changes in cell size in parallel to measuring changes in chloride flux. As measured by flow cytometry, after 2 hours of treatment, ivermectin caused an increase in cell size in OCI-AML2 but not in the resistant DU145 cells, consistent with its effects on chloride influx (Figure 3D-E).

In nematodes, increases in intracellular chloride after ivermectin treatment cause membrane hyperpolarization. Therefore, we evaluated the effects of ivermectin on plasma and mitochondrial membrane polarization in leukemia cells. OCI-AML2, U937, and TEX leukemia cells sensitive to ivermectin-induced death, a primary AML patient sample, DU145 and PPC-1 prostate cancer cells, and primary normal hematopoietic cells were treated with increasing concentrations of ivermectin. At increasing times after incubation, plasma membrane potential was measured by staining cells with DiBAC4(3) and flow cytometric analysis. In OCI-AML2 cells, treatment with ivermectin induced membrane hyperpolarization in a dose-dependent manner (Figure 4A) and as early as after 1

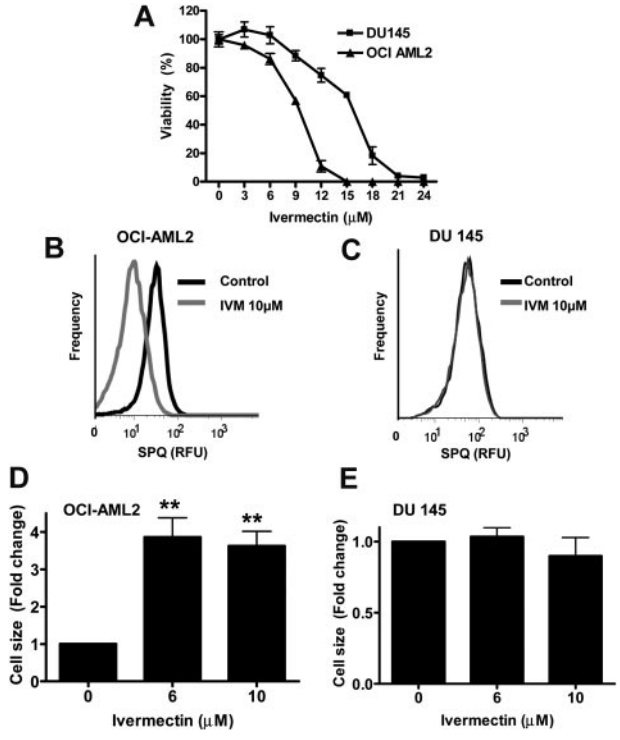

Figure 3. Ivermectin induces chloride influx and increases cell size in leukemia cells. (A) OCI-AML2 leukemia and DU145 prostate cancer cells were treated with increasing concentrations of ivermectin. After 24 hours of incubation, cell growth and viability were measured by MTS assay. Data represent the mean ± SD percent viable cells from representative experiments. (B) OCI-AML2 and (C) DU145 cells were treated with 10μM ivermectin for 1 hour, and levels of intracellular chloride were measured after staining cells with the fluorescent dye, SPQ, that is quenched by high chloride ion concentrations. Histograms from representative experiments are shown. (D) OCI-AML2 and (E) DU145 cells were treated with 6 and 10μM ivermectin for 1 hour. After treatment, cell size was measured by forward light scatter and flow cytometry. Data represent mean ± SD fold change in cell size compared with control from representative experiments performed in triplicate. **$P < .01$, by unpaired *t* test.

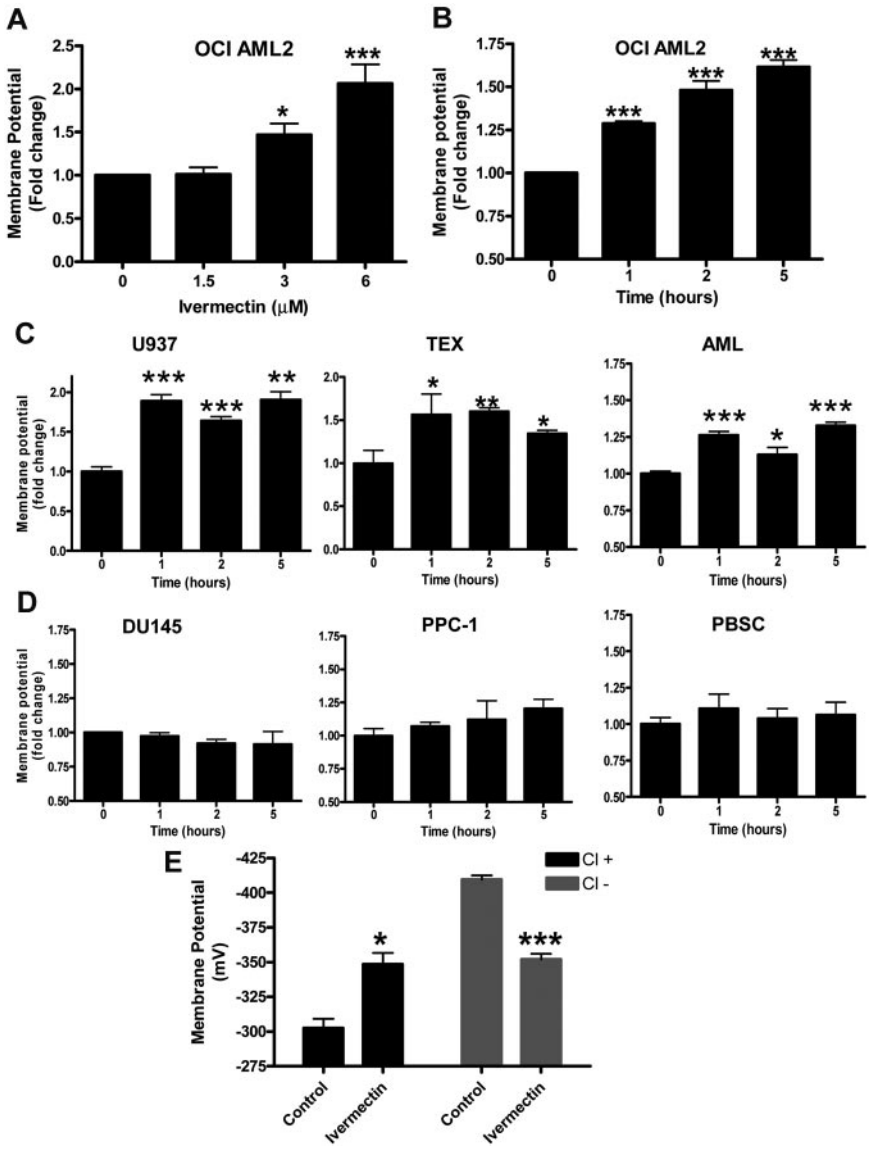

Figure 4. Ivermectin induces plasma membrane hyperpolarization dependent on chloride influx. OCI-AML2 cells were treated with increasing concentrations of ivermectin for 24 hours (A) or 6μM ivermectin for increasing times of incubation (B). After treatment, plasma membrane potential was measured by staining cells with DiBAC4(3) and flow cytometric analysis. Data represent the mean ± SD fold change in plasma membrane potential compared with control treated cells. Representative experiments performed in triplicate are shown. Differences in change of membrane potential compared with control were analyzed by an unpaired *t* test. ***$P < .001$; *$P < .05$. U937 and TEX leukemia cells, a primary AML sample (AML), (C) DU145 and PPC-1 prostate cancer, and 2 samples of normal hematopoietic cells (D) were treated with 6μM ivermectin for increasing times. After treatment, plasma membrane potential was measured as described above. Data represent the mean ± SD fold change in plasma membrane potential compared with control treated cells. Representative experiments performed in triplicate are shown. Differences in change of membrane potential, compared with control, were analyzed by an unpaired *t* test. ***$P < .001$; *$P < .05$. (E) OCI-AML2 cells were treated with 6μM ivermectin in chloride-replete and chloride-free media for 5 hours. After incubation, plasma membrane potential was measured as described above. Data represent the mean ± SD change in plasma membrane potential, compared with untreated cells in chloride-replete media. Representative experiments performed in triplicates are shown. Differences in change of membrane potential, compared with control, were analyzed by an unpaired *t* test. ***$P < .001$; *$P < .05$.

hour of treatment (Figure 4B), consistent with the influx of intracellular chloride and the effects observed in nematodes. Likewise, U937 and TEX leukemia cells, as well as primary AML cells sensitive to ivermectin-induced death, also demonstrated plasma membrane hyperpolarization after ivermectin treatment (Figure 4C). In contrast, DU145 and PPC-1 cells, as well as primary normal hematopoietic cells that were more resistant to ivermectin, did not show changes in their plasma membrane potential when treated with up to 6μM ivermectin for up to 24 hours (Figure 4D).

To determine whether the plasma membrane hyperpolarization observed after ivermectin treatment was related to increased chloride ion flux, we measured plasma membrane polarization after treating cells with ivermectin in buffers with and without chloride. OCI-AML2 cells were treated for 5 hours with ivermectin in a chloride-replete buffer or a chloride-free buffer, where sodium and potassium chloride were replaced with equimolar gluconate salts of sodium and potassium. When added to cells in the chloride-replete buffer, ivermectin induced plasma membrane hyperpolarization similar to cells treated in RPMI medium. However, when added to cells in chloride-free buffer, ivermectin caused plasma membrane depolarization (Figure 4E). Thus, the effects of ivermectin on plasma membrane polarization appear to be related to increased chloride flux.

Ivermectin increases intracellular calcium but is not functionally relevant in leukemia cells

Plasma membrane hyperpolarization can lead to calcium influx.[18] Therefore, we tested the effects of ivermectin on calcium influx in leukemia cells. OCI-AML2 cells were treated with ivermectin and the concentration of intracellular calcium was measured by staining cells with the ratiometric dye, Indo-1 AM. As a positive control, cells were treated with digoxin, which is known to increase intracellular calcium.[19,20] Similar to the effects of digoxin, ivermectin increased intracellular calcium (supplemental Figure 4A-B). However, the increase in intracellular calcium did not appear sufficient to explain the cytotoxicity of ivermectin, because chelation of intra- and extracellular calcium with BAPTA-AM and EDTA (ethylenediaminetetraacetic acid), respectively, did not inhibit ivermectin-induced cell death (data not shown).

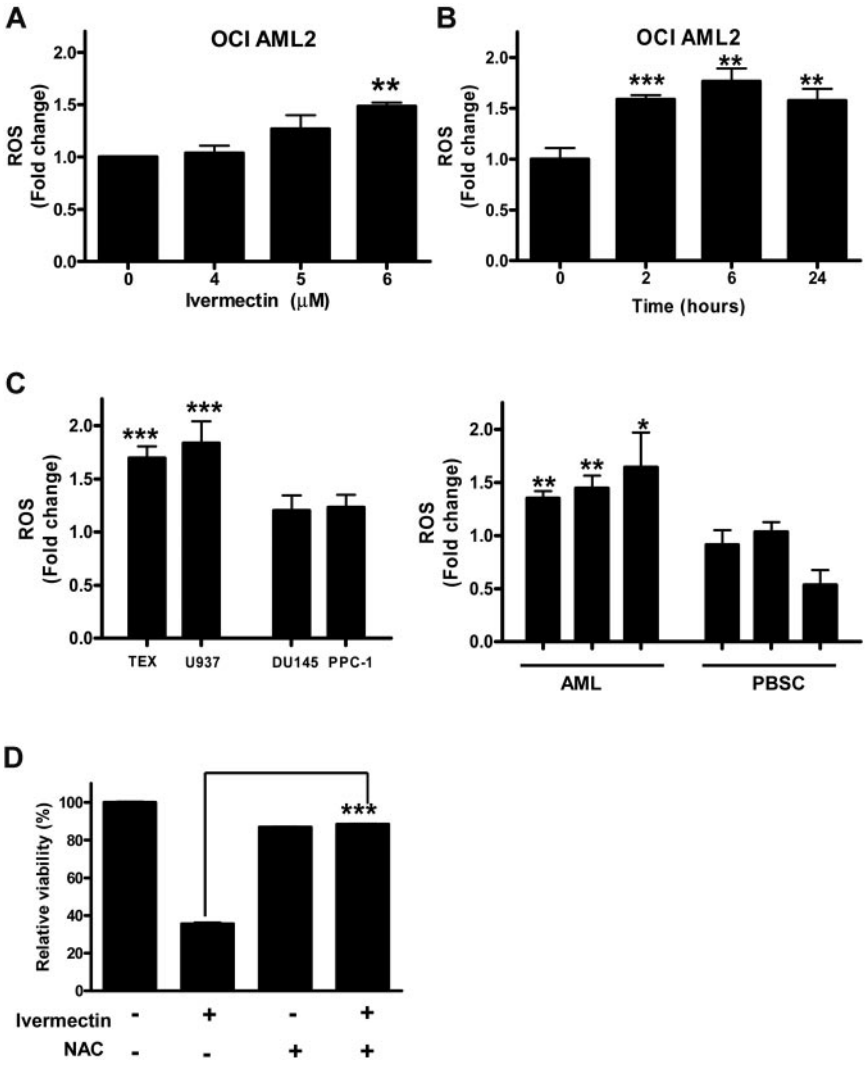

Figure 5. Ivermectin induces generation of ROS. OCI-AML 2 leukemia cells were treated with increasing concentrations of ivermectin overnight (A) or 6μM ivermectin for increasing incubation times (B). After incubation, ROS was detected by staining cells with Carboxy-H_2DCFDA (final concentration 10μM) and flow cytometric analysis. Data represent the mean ± SD fold change in ROS production, compared with control. Representative experiments performed in triplicate are shown. Differences in change of ROS compared with control were analyzed by an unpaired *t* test. ***$P < .001$; **$P < .005$. (C) U937 and TEX leukemia cells and DU145 and PPC-1 prostate cells were treated with ivermectin at 6μM for 2 hours. After treatment, ROS generation was measured as described above. Data represent the mean ± SD fold change in ROS production compared with each of their buffer treated controls. Representative experiments performed in triplicate are shown. Differences in change of ROS compared with control were analyzed by an unpaired *t* test. ***$P < .001$. Primary AML cells (n = 3) and normal hematopoietic stem cells (PBSCs, n = 3) were treated with ivermectin (6μM) for 6 hours. After treatment, ROS generation was measured as described above. Data represent the mean ± SD fold change in ROS production compared with each of their buffer treated controls for experiments performed in triplicate. Differences in ROS production compared with control were analyzed by an unpaired *t* test. ***$P < .001$. (D) OCI-AML2 cells were treated simultaneously with ivermectin (3μM), the ROS scavenger, NAC (5μM), or the combination of NAC and ivermectin. After 48 hours of treatment, cell growth and viability were measured by the MTS assay. Data represent the mean ± SD percent viable cells from a representative experiment performed in triplicate. Differences in change of cell viability, compared with control, were analyzed by an unpaired *t* test. ***$P < .001$.

Ivermectin increases intracellular ROS

Manganese chloride, cobalt chloride, and mercuric chloride can lead to generation of ROS.[21-23] Therefore, we tested whether ivermectin increased ROS production in leukemia cells due to the observed chloride influx. OCI-AML2 cells were treated with ivermectin at increasing concentrations and times of incubation. After treatment, levels of intracellular ROS were measured by staining cells with Carboxy-H_2DCFDA and flow cytometry. Treatment with ivermectin increased ROS production at times and concentrations that coincided with plasma membrane hyperpolarization (Figure 5A-B). Likewise, U937 and TEX leukemia cells that were sensitive to ivermectin-induced death demonstrated increased ROS generation 2 hours after ivermectin treatment (Figure 5C). In contrast, DU145 and PPC-1 cells that were more resistant to ivermectin did not show changes in ROS generation. Likewise, primary AML cells, but not normal hematopoietic cells, demonstrated increased ROS generation after ivermectin treatment (Figure 5C).

To determine whether the increased ROS production was functionally important for ivermectin-induced cell death, cells were treated simultaneously with ivermectin along with the free radical scavenger *N*-acetyl-L-cysteine (NAC). NAC abrogated ivermectin-induced cell death consistent with a mechanism of cell death related to ROS production and in keeping with its effects on plasma membrane hyperpolarization and chloride influx (Figure 5D).

Changes in ROS production are indicative of a biologic response to ivermectin, but are very difficult to measure in the context of a clinical trial. Therefore, to identify alterations in gene expression that are a result of ROS production and could be used as biomarkers in the context of a clinical trial, we undertook gene expression profiling analysis (using Affymetrix HG U133 Plus 2.0 arrays) of RNA derived from OCI-AML2 cells treated with ivermectin for 30 and 40 hours (supplemental Table 1). One hundred fifty genes were deregulated > 4-fold at both time points (33 underexpressed; 117 overexpressed), compared with control. Among these genes dysregulated were *STAT1*, which has been associated with increased ROS generation[24-26] and the STAT1 downstream targets, *IFIT3*, *OAS1*, and *TRIM22*. We validated the up-regulation of *STAT1* and target genes *IFIT3*, *OAS1*, and *TRIM22* after ivermectin treatment by qRT-PCR, (Figure 6A). Likewise, U937 and HL60 leukemia cells that were sensitive to ivermectin-induced death also demonstrated increased *STAT1* mRNA. In contrast, DU145 and PPC-1 cells that were more resistant to ivermectin did not show changes in *STAT1* expression (Figure 6B). We also evaluated changes in *STAT1* expression in tumors from a leukemia xenograft model. Mice with OCI-AML2 subcutaneous xenografts were treated with ivermectin for 5 days. After treatment, tumors were

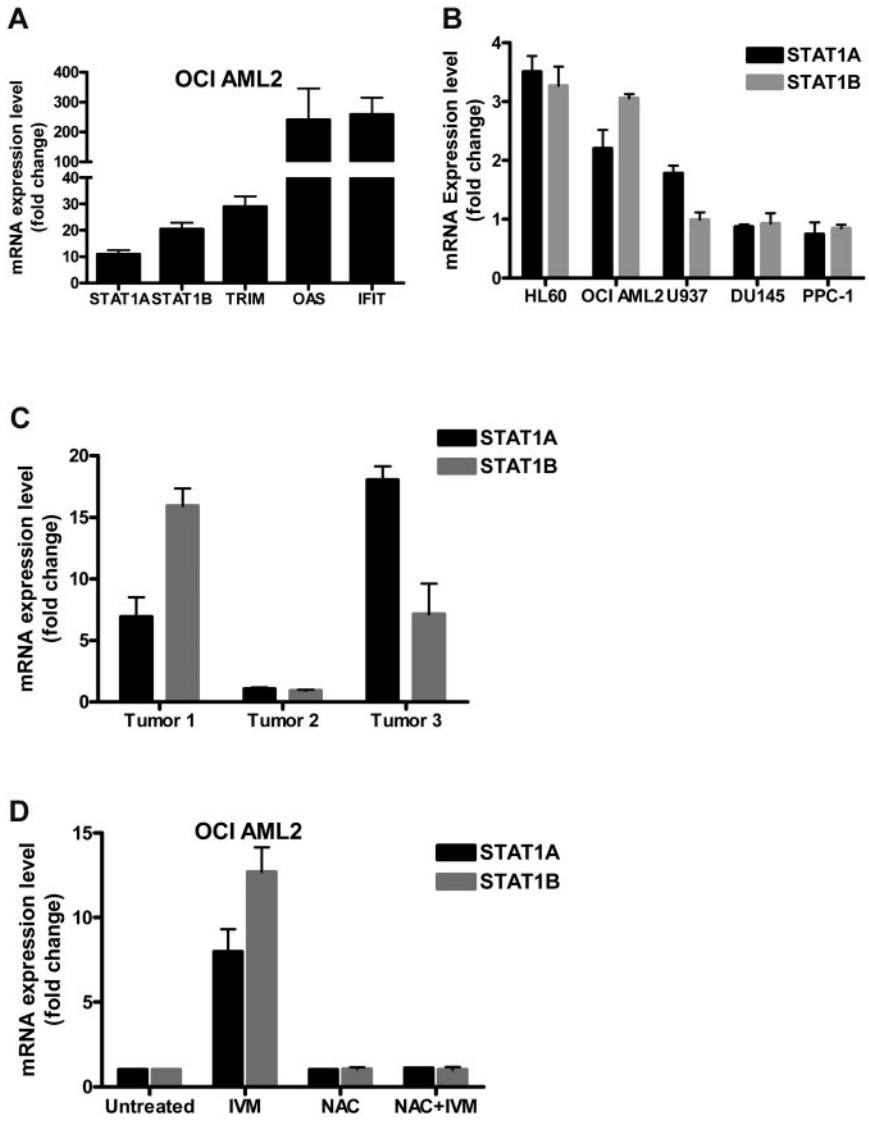

Figure 6. Ivermectin increases expression of STAT1 and its target genes through a ROS-dependent mechanism. (A) OCI-AML2 cells were treated with 3μM ivermectin (IVM) for 30 hours. After treatment, RNA was isolated, reverse transcribed, and subjected to quantitative PCR using specific primers for *STAT1A, STAT1B*, and STAT1 target genes *OAS1, TRIM22*, and *IFIT3*. Data represent mean ± SD fold increase in gene expression normalized to 18S expression and compared with control cells. (B) OCI AML2, U937, and HL60 leukemia and DU145 and PPC-1 prostate cancer cells were treated with 6μM ivermectin for 24 hours, and mRNA levels of *STAT1A* and *STAT1B* were measured using qPCR and normalized to 18S expression as (A). Data represent mean ± SD fold increase in gene expression, compared with control cells. (C) OCI-AML2 cells (2.5×10^5) were injected subcutaneously into the flanks of sublethally irradiated NOD/SCID mice. Once tumors were established, mice were treated with ivermectin (7 mg/kg) intraperitoneally or vehicle control for 5 days (n = 3 per group). After treatment, mice were killed, and tumors were harvested. mRNA was extracted, and changes in *STAT1A* and *1B* expression were measured by qRT-PCR. Data represent mean ± SD fold increase in gene expression normalized to 18S expression, compared with tumors from control treated mice. (D) OCI-AML2 cells were treated simultaneously with ivermectin (3μM), the ROS scavenger, NAC (5μM), or both for 30 hours, and *STAT1A* and *STAT1B* expression was assessed as described for panel A. Relative expression values normalized to 18s are reported as fold-change ± SD compared with the untreated control for each gene.

harvested, mRNA was extracted, and *STAT1* expression was measured by qRT-PCR. *STAT1* mRNA was increased in 2 of 3 tested tumors from mice treated with ivermectin, compared with *STAT1* mRNA expression from tumors harvested from mice treated with vehicle control (Figure 6C). We also demonstrated that changes in *STAT1* genes were secondary to ROS production as pretreatment with NAC blocked their up-regulation (Figure 6D).

Of note, we also compared our array dataset to a ROS gene signature reported by Tothova et al.[27] Of the 55 genes in the Tothova signature, two-thirds were present in our dataset. Of these 36 genes, 55% (20 genes) were found to be differentially regulated on ivermectin treatment (fold-change of 1.25 up or down, compared with the untreated control sample). Thus, ivermectin appears to induce genetic changes consistent with ROS induction.

Ivermectin synergizes with cytarabine and daunorubicin

Cytarabine and daunorubicin increase ROS production through mechanisms related to DNA damage (Figure 7A-B) and are used clinically in the treatment of AML.[28,29] Therefore, we evaluated the effects of the combination of ivermectin with cytarabine and daunorubicin on cell viability. OCI-AML2 and U937 cells were treated with increasing concentrations of ivermectin alone and in combination with cytarabine and daunorubicin. Cell growth and viability were measured 72 hours after incubation using the MTS assay. Data were analyzed by the CalcuSyn median effect model, where the CI indicates synergism (CI < 0.9), additivity (CI = 0.9-1.1) or antagonism (CI > 1.1). In both OCI-AML2 and U937 leukemia cells, the combination of ivermectin and cytarabine demonstrated strong synergism, with CI values at the ED_{25}, ED_{50}, and ED_{75} of 0.51, 0.58, and 0.65, respectively, in OCI AML2 cells and ED_{25}, ED_{50}, and ED_{75} of 0.55, 0.71, and 0.91 in U937 cells (Figure 7C). Likewise, in OCI-AML2 cells, the combination of ivermectin and daunorubicin was also synergistic, with CI values at the ED_{25}, ED_{50}, and ED_{75} of 0.48, 0.51, and 0.54, respectively. In contrast, the combination of ivermectin and daunorubicin was closer to the additive in U937, with CI values at the ED_{25}, ED_{50}, and ED_{75} of 1.1, 0.98, and 0.85, respectively (Figure 7D).

We also tested the combination of ivermectin and cytarabine in normal hematopoeitic cells. In contrast to the effects observed in the leukemia cell lines, ivermectin did not enhance the cytotoxicity of cytarabine in normal cells (Figure 7E).

Drug sequencing can affect the activity of drug combinations. Therefore, we tested the effect of drug sequencing on the synergism

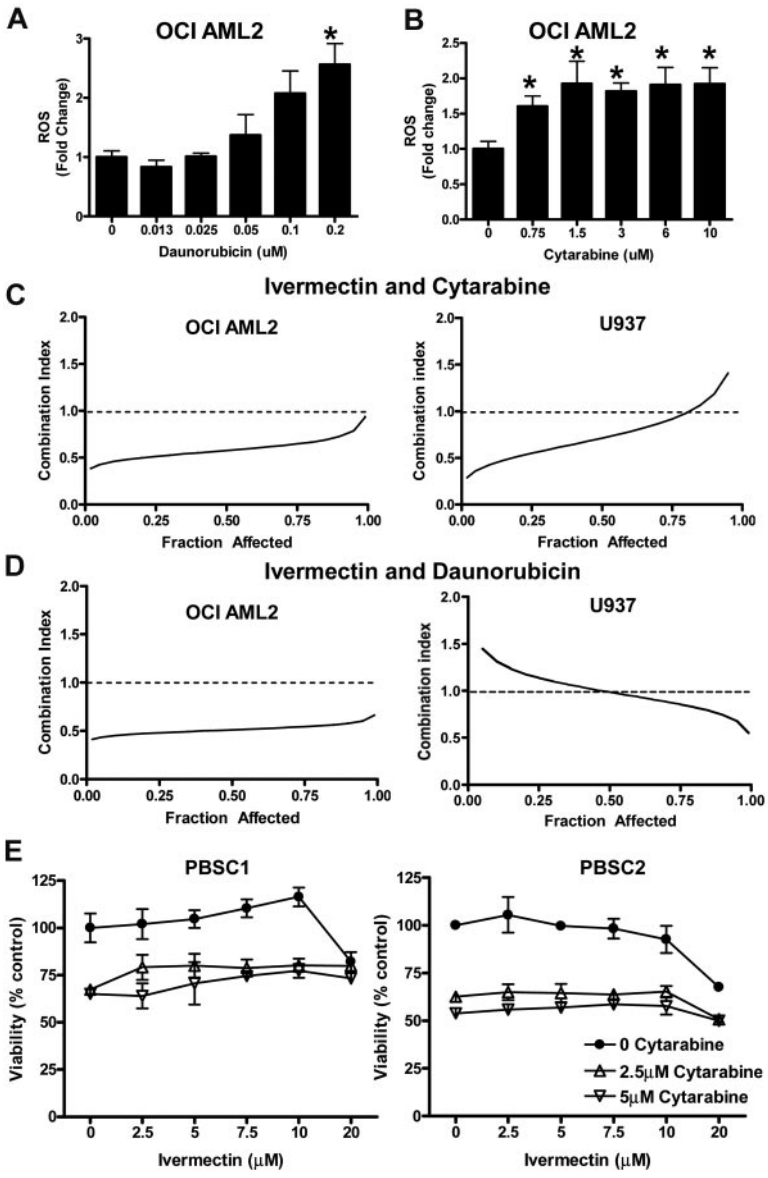

Figure 7. Ivermectin synergizes with cytarabine and daunorubicin to induce cell death in leukemia cells. OCI-AML2 cells were treated with increasing concentrations of daunorubicin (A) and cytarabine (B) overnight. After treatment, ROS was measured by staining cells with Carboxy-H_2DCFDA (final concentration 10μM) and flow cytometric analysis. Data represent the mean ± SD fold change in ROS production compared with control. Representative experiments performed in triplicate are shown. The effects of different concentrations of ivermectin in combination with cytarabine and daunorubicin on the viability of OCI-AML2 and U937 cells were measured by MTS assay after 72 hours of incubation. Data were analyzed with CalcUSyn software as described in Methods. CI versus Fractional effect (Fa) plot showing the effect of the combination of ivermectin with cytarabine (C) and ivermectin with daunorubicin (D) in OCI AML2 and U937 are illustrated in the isobolograms. CI < 0.9 indicates synergism. Representative isobolograms of experiments performed in triplicate are shown. (E) Normal hematopoietic cells (PBSCs; n = 2) were treated with T increasing concentrations of ivermectin and cytarabine (0, 2.5, and 5μM). After 48 hours, cell viability was measured by annexin V–PI staining. Data represent the mean ± SD percent of viable cells from experiments performed in triplicate.

between ivermectin and cytarabine or daunorubicn. In OCI-AML2 and U937 cells, the combination of ivermectin and cytarabine remained synergistic, regardless of whether the ivermectin was given with, before, or after the addition of cytarabine (Figure 7F). In contrast, in OCI-AML2 cells, the combination of ivermectin was synergistic when given before or simultaneously with daunorubicin. However, the effects of the combination were additive when the ivermectin was given after the addition of daunorubicin. (Figure 7F)

We also evaluated the combination of ivermectin with the anthelmintic agent, albendazole, as this agent synergized with ivermectin in the treatment of nematodes.[30,31] In contrast to the synergy observed with cytarabine and daunorubicin, albendazole antagonized the antileukemic effects of ivermectin, with CI values at the ED_{25}, ED_{50}, and ED_{75} of 1.59, 1.09, and 0.89, respectively (data not shown).

Discussion

To identify known drugs with previously unrecognized antileukemia activity, we compiled and screened a library of off- and on-patent drugs for compounds cytotoxic to leukemia cells. From this screen, we identified the antiparasitic agent, ivermectin, which induced cell death in leukemia cell lines at low micromolar concentrations and delayed tumor growth in mouse models of leukemia.

As part of its development as an antiparasitic agent, the pharmacology and toxicology of ivermectin have been studied extensively in humans and animals. Humans treated for onchocerciasis typically receive a single dose of 100-200 μg/kg ivermectin to eradicate the parasite. In such patients, plasma concentration of 52.0 ng/mL have been achieved in 5.2 hours, with an area under the curve over 48 hours of 2852 ng • h/mL.[32] Similar pharmacokinetics have been reported in healthy male volunteers receiving a 14-mg capsule of radiolabeled ivermectin. In these subjects, the mean T_{max} was 6 hours, with a half-life of 11.8 hours.[10] These doses of ivermectin produce plasma levels that are likely lower than the concentrations required to induce an antileukemic effect and may explain why antitumor effects of ivermectin have not been previously reported in patients receiving standard doses of this drug for the treatment of onchocerciasis. However, higher concentrations of ivermectin that may possess antitumor activity have been well tolerated in both humans and animals. For example, the LD_{50} of oral ivermectin is

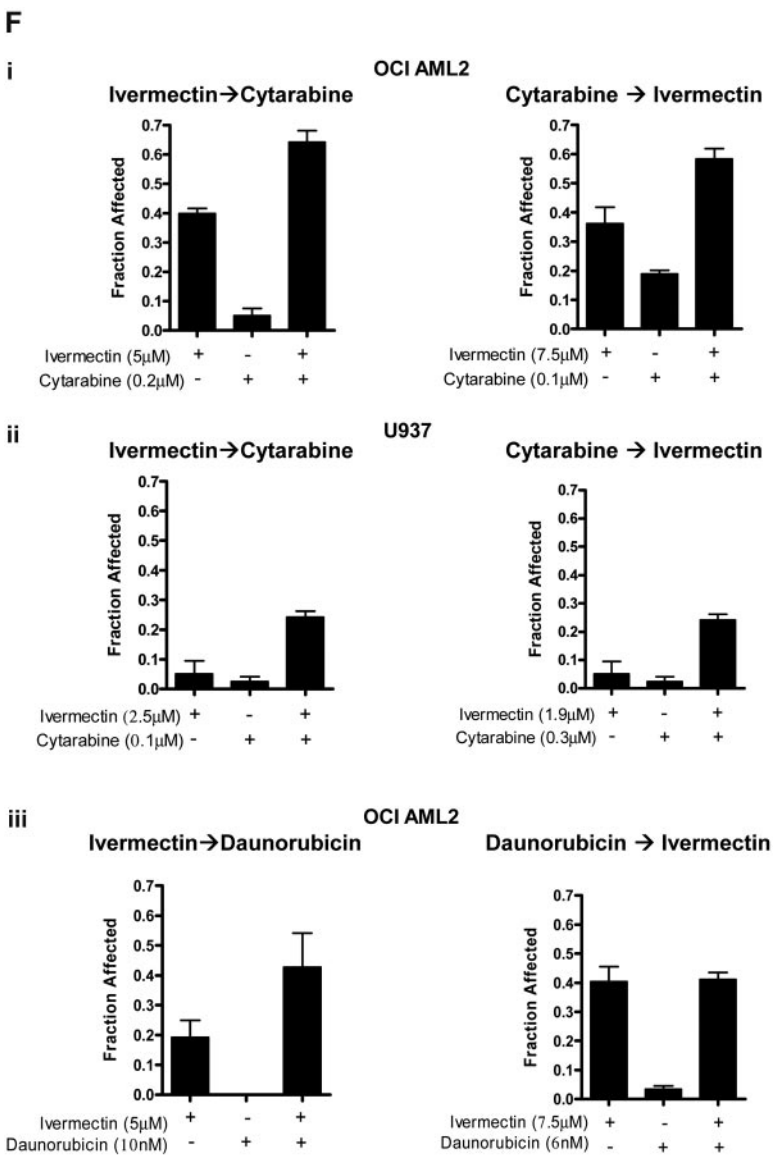

Figure 7 (continued). (F) OCI-AML2 (i) and U937 (ii) cells were treated with ivermectin, cytarabine, or the combination of the 2 drugs at varying concentrations for 72 hours. Ivermectin→cytarabine denotes that ivermectin was added initially, and cytarabine was added for the last 48 hours of the 72-hour experiment. Cytarabine→ivermectin denotes that cytarabine was added initially, and ivermectin was added for the last 48 hours of the 72-hour experiment. OCI-AML2 (iiii) cells were treated with ivermectin, daunorubicin, or the combination of the 2 drugs at varying concentrations for 72 hours. Ivermectin→daunorubicin denotes that ivermectin was added initially, and the daunorubicin was added for the last 48 hours of the 72-hour experiment. Daunorubicin→ivermectin denotes that daunorubicin was added initially, and the ivermectin was added for the last 48 hours of the 72-hour experiment. After treatment, cell growth and viability was measured by the MTS assay. Representative experiments performed in triplicate are shown. Data represent mean ± SD fractional effect (cell death).

approximately 28-30 mg/kg in mice, 80 mg/kg in dogs, and above 24 mg/kg in monkeys.[7,32] Humans with spinal injury and muscle spasticity have been treated with up to 1.6 mg/kg of ivermectin subcutaneously twice weekly for up to 12 weeks without toxicity.[9] In addition, reports of ivermectin overdoses also support the potential wide therapeutic window of this drug. For example, an individual who self-administered 6 g of veterinary ivermectin 30-50 times over the course of 1 year had no evidence of toxicity from the ivermectin.[11] Multiple other ingestion events have also been reported, particularly in pediatric subjects who accidentally consumed veterinary ivermectin kept in the household for the family dog. In the majority of these, no serious adverse events were reported.[9,11]

Although no prior clinical studies have directly evaluated ivermectin as an anticancer agent, a case report suggests that ivermectin may have activity in the treatment of leukemia.[33] An adult male with T-cell leukemia/lymphoma presented with a generalized pruritic, erythrodermic rash with areas of hyperkeratosis and was diagnosed with scabies. He received 200 μg/kg ivermectin on days 1 and 10 with complete resolution of the rash. While not a focus of the paper, it is possible that a component of the patient's rash may have been due to leukemia and this rash responded to ivermectin. Moreover, the leukemia cells in the peripheral blood were controlled while receiving ivermectin

Our studies suggest that ivermectin induces cell death through a mechanism related to its known function as an activator of chloride channels. As an antiparasitic agent, ivermectin activates glutamate-gated chloride channels unique to invertebrates. However, at higher concentrations, ivermectin also activates mammalian chloride channels.[7] Mammalian chloride channels broadly fall into 5 classes, based on their regulation: cystic fibrosis transmembrane conductance regulator, which is activated by cyclic AMP dependent phosphorylation; calcium-activated chloride channels; voltage-gated chloride channels (ClCs); ligand-gated chloride channels (γ-aminobutyric acid and glycine-activated); and volume-regulated chloride channels. These channels act in heteromeric complexes dependent upon cell type, with many possible permutations and combinations of the subunits.[34] Currently, it is unclear which mammalian chloride channels are being activated by ivermectin, but the complexity of their organization makes it difficult to identify single "target" channels for ivermectin activity using standard genetic experiments.

The short-term cytotoxicity studies and the in vivo experiments support a therapeutic window for ivermectin as an antileukemia agent, but the difference between normal $CD34^+$ cells and malignant cells was narrower, as were the differences in the clonogenic growth assays. However, it is important to note that results of these assays do not always predict clinical toxicity. For example, cytarabine and amsacrine are chemotherapeutic agents routinely used in the treatment of AML, but show little or no selectivity for malignant cells over normal cells in colony formation assays.[35,36] In addition, we demonstrated that oral ivermectin delayed tumor growth in 3 mouse models of leukemia without untoward toxicity, supporting a therapeutic window. Finally, toxicology studies with ivermectin in animals and humans did not report hematologic toxicity. Nonetheless, the small differential sensitivity between primary AML and normal hematopoietic cells raises concerns about the potential hematologic toxicity, and its safety will have to be carefully evaluated in phase 1 clinical trials.

The basis for the therapeutic window after invermectin treatment is likely multifactorial. Chloride channels are often increased on the surface of malignant cells, compared with normal cells, potentially making them more sensitive to alterations in chloride flux by ivermectin. For example, compared with normal neutrophils, HL60 cells overexpress the ClC-5 chloride channel that is normally expressed in renal cells.[37] In support of this mechanism, we observed less chloride flux in cells more resistant to ivermectin. Alterations in intracellular chloride concentrations also affect basic homeostatic parameters, such as intracellular Ca^{2+} levels, pH, and cell volume,[38] and alteration of these parameters can induce apoptosis.[39] Finally, the therapeutic window with ivermectin treatment may reflect differences in sensitivity to ROS generation. Ivermectin increased ROS generation that appeared functionally important for its cytotoxicity, and previous studies support a mechanism of ROS generation related to increased chloride influx.[22,40-42] Previous studies have also demonstrated that malignant cells have higher basal levels of ROS and are less tolerant of ROS-inducing agents, compared with normal cells.[43,44] Future studies will help clarify the basis of the therapeutic window as well as identify subgroups of patients most likely to respond to this therapy.

Cytarabine and daunorubicin, which are used in the treatment of AML, induce ROS generation through a mechanism linked to DNA damage and thus a mechanism distinct from ivermectin. Consequently, we evaluated the combination of these drugs with ivermectin and demonstrated synergy with both of these drugs. Therefore, ivermectin could be evaluated in combination with these agents to enhance the efficacy of standard therapy for AML.

In summary, we have shown that ivermectin induces cell death in leukemia cells via chloride influx, membrane hyperpolarization, and increasing levels of intracellular ROS. Given its prior safety record in humans and animals coupled with its preclinical efficacy in leukemia, a phase 1 clinical trial could be conducted to determine the tolerance and biologic activity of oral ivermectin in these patients.

Acknowledgments

A.D.S. is a Leukemia & Lymphoma Society Scholar in Clinical Research. M.A.S. is a Canadian Institutes of Health Research postdoctoral fellow, and holds a postdoctoral research fellowship from the Multiple Myeloma Research Foundation and Millennium Pharmaceuticals. M.S. is a Canadian Institutes of Health Research Banting and Best Canada Graduate Scholar.

Authorship

Contribution: S.S. designed research, analyzed data, performed research, and wrote the paper; M.S. designed research, analyzed data, and performed research; M.A.S. designed research, analyzed data, and performed research; R.H. performed research and analyzed data; M.G. performed research and analyzed data; X.W. performed research and analyzed data; S.B.F. performed research and analyzed data; H.S. performed research and analyzed data; T.E.W. designed research, analyzed data, and performed research; R.W. performed research and analyzed data; M.D.M. contributed critical reagents and analyzed data; R.A.B. designed research and supervised research,; A.D. designed research, preformed research, and analyzed data; J.W. and S.O.K. supervised research; A.D.S. designed research, analyzed data, supervised research, and wrote the manuscript; and all authors reviewed and edited the paper.

Conflict-of-interest disclosure: The authors declare no competing financial interests.

Correspondence: Aaron D. Schimmer, Princess Margaret Hospital, Ontario Cancer Institute, 610 University Ave, Toronto, ON, Canada, M5G 2M9; e-mail: aaron.schimmer@utoronto.ca.

References

1. Tan K, Culjkovic B, Amri A, Borden KL. Ribavirin targets eIF4E dependent Akt survival signaling. *Biochem Biophys Res Commun.* 2008;375(3):341-345.
2. Kentsis A, Topisirovic I, Culjkovic B, Shao L, Borden KL. Ribavirin suppresses eIF4E-mediated oncogenic transformation by physical mimicry of the 7-methyl guanosine mRNA cap. *Proc Natl Acad Sci U S A.* 2004;101(52):18105-18110.
3. Assouline S, Culjkovic B, Cocolakis E, et al. Molecular targeting of the oncogene eIF4E in acute myeloid leukemia (AML): a proof-of-principle clinical trial with ribavirin. *Blood.* 2009;114(2):257-260.
4. Sella A, Kilbourn R, Amato R, et al. Phase II study of ketoconazole combined with weekly doxorubicin in patients with androgen-independent prostate cancer. *J Clin Oncol.* 1994;12(4):683-688.
5. Small EJ, Halabi S, Dawson NA, et al. Antiandrogen withdrawal alone or in combination with ketoconazole in androgen-independent prostate cancer patients: a phase III trial (CALGB 9583). *J Clin Oncol.* 2004;22(6):1025-1033.
6. Mao X, Li X, Sprangers R, et al. Clioquinol inhibits the proteasome and displays preclinical activity in leukemia and myeloma. *Leukemia.* 2009;23(3):585-590.
7. Dadarkar SS, Deore MD, Gatne MM. Comparative evaluation of acute toxicity of ivermectin by two methods after single subcutaneous administration in rats. *Regul Toxicol Pharmacol.* 2007;47(3):257-260.
8. Brown KR, Ricci FM, Ottesen EA. Ivermectin: effectiveness in lymphatic filariasis. *Parasitology.* 2000;121(suppl):S133-S146.
9. Costa JL, Diazgranados JA. Ivermectin for spasticity in spinal-cord injury. *Lancet.* 1994;343(8899):739.
10. Guzzo CA, Furtek CI, Porras AG, et al. Safety, tolerability, and pharmacokinetics of escalating high doses of ivermectin in healthy adult subjects. *J Clin Pharmacol.* 2002;42(10):1122-1133.
11. Frost M. FDA new drug application (NDA) for STROMECTOL (ivermectin) 6-mg for the treatment of strongyloidiasis and onchocerciasis. 1996.
12. Pilas B, Durack G. A flow cytometric method for measurement of intracellular chloride concentration in lymphocytes using the halide-specific probe 6-methoxy-N-(3-sulfopropyl) quinolinium (SPQ). *Cytometry.* 1997;28(4):316-322.
13. Gurfinkel DM, Chow S, Hurren R, et al. Disruption of the endoplasmic reticulum and increases in cytoplasmic calcium are early events in cell death induced by the natural triterpenoid, Asiatic acid. *Apoptosis.* 2006;11(9):1463-1471.
14. Pham NA, Jacobberger JW, Schimmer AD, Cao P, Gronda M, Hedley DW. The dietary isothiocyanate, sulforaphane, targets pathways of apoptosis, cell cycle arrest, and oxidative stress in human pancreatic cancer cells and inhibits tumor growth in severe combined immunodeficient mice. *Mol Cancer Ther.* 2004;3(10):1239-1248.
15. Eberhard Y, McDermott SP, Wang X, et al.

Chelation of intracellular iron with the antifungal agent, ciclopirox olamine, induces cell death in leukemia and myeloma cells. *Blood.* 2009; 114(14):3064-3073.

16. Chou TC, Talalay P. Quantitative analysis of dose-effect relationships: the combined effects of multiple drugs or enzyme inhibitors. *Adv Enzyme Regul.* 1984;22:27-55.
17. Gonzalez Canga A, Sahagun Prieto AM, Diez Liebana MJ, Fernandez Martinez N, Sierra Vega M, Garcia Vieitez JJ. The pharmacokinetics and interactions of ivermectin in humans—a mini-review. *AAPS J.* 2008;10(1):42-46.
18. McCarty MF, Barroso-Aranda J, Contreras F. The hyperpolarizing impact of glycine on endothelial cells may be anti-atherogenic. *Med Hypotheses.* 2009;73(2):263-264.
19. Meral I, Hsu W, Hembrough FB. Digoxin- and monensin-induced changes of intracellular Ca2+ concentration in isolated guinea-pig ventricular myocyte. *J Vet Med A Physiol Pathol Clin Med.* 2002;49(6):329-333.
20. Wagner J, Bremhorst T, Schumann HJ. Influence of frequency of stimulation on the toxicity of digoxin on isolated guinea-pig atria in different extracellular Ca2+. *Arch Int Pharmacodyn Ther.* 1978;236(2):228-233.
21. Park EJ, Park K. Induction of reactive oxygen species and apoptosis in BEAS-2B cells by mercuric chloride. *Toxicol In Vitro.* 2007;21(5):789-794.
22. Zhang P, Hatter A, Liu B. Manganese chloride stimulates rat microglia to release hydrogen peroxide. *Toxicol Lett.* 2007;173(2):88-100.
23. Kamiya T, Hara H, Yamada H, Imai H, Inagaki N, Adachi T. Cobalt chloride decreases EC-SOD expression through intracellular ROS generation and p38-MAPK pathways in COS7 cells. *Free Radic Res.* 2008;42(11-12):949-956.
24. Kim HS, Cho IH, Kim JE, et al. Ethyl pyruvate has an anti-inflammatory effect by inhibiting ROS-dependent STAT signaling in activated microglia. *Free Radic Biol Med.* 2008;45(7):950-963.
25. Kim HS, Lee MS. Essential role of STAT1 in caspase-independent cell death of activated macrophages through the p38 mitogen-activated protein kinase/STAT1/reactive oxygen species pathway. *Mol Cell Biol.* 2005;25(15):6821-6833.
26. Liu T, Castro S, Brasier AR, Jamaluddin M, Garofalo RP, Casola A. Reactive oxygen species mediate virus-induced STAT activation: role of tyrosine phosphatases. *J Biol Chem.* 2004; 279(4):2461-2469.
27. Tothova Z, Kollipara R, Huntly BJ, et al. FoxOs are critical mediators of hematopoietic stem cell resistance to physiologic oxidative stress. *Cell.* 2007;128(2):325-339.
28. Tsang WP, Chau SP, Kong SK, Fung KP, Kwok TT. Reactive oxygen species mediate doxorubicin induced p53-independent apoptosis. *Life Sci.* 2003; 73(16):2047-2058.
29. Iacobini M, Menichelli A, Palumbo G, Multari G, Werner B, Del Principe D. Involvement of oxygen radicals in cytarabine-induced apoptosis in human polymorphonuclear cells. *Biochem Pharmacol.* 2001;61(8):1033-1040.
30. Asio SM, Simonsen PE, Onapa AW. Mansonella perstans: safety and efficacy of ivermectin alone, albendazole alone, and the two drugs in combination. *Ann Trop Med Parasitol.* 2009;103(1):31-37.
31. Demeler J, Van Zeveren AM, Kleinschmidt N, et al. Monitoring the efficacy of ivermectin and albendazole against gastro intestinal nematodes of cattle in Northern Europe. *Vet Parasitol.* 2009; 160(1-2):109-115.
32. Baraka OZ, Mahmoud BM, Marschke CK, Geary TG, Homeida MM, Williams JF. Ivermectin distribution in the plasma and tissues of patients infected with Onchocerca volvulus. *Eur J Clin Pharmacol.* 1996;50(5):407-410.
33. Yonekura K, Kanekura T, Kanzaki T, Utsunomiya A. Crusted scabies in an adult T-cell leukemia/lymphoma patient successfully treated with oral ivermectin. *J Dermatol.* 2006;33(2):139-141.
34. Verkman AS, Galietta LJ. Chloride channels as drug targets. *Nat Rev Drug Discov.* 2009;8(2): 153-171.
35. Singer CR, Linch DC. Comparison of the sensitivity of normal and leukaemic myeloid progenitors to in-vitro incubation with cytotoxic drugs: a study of pharmacological purging. *Leuk Res.* 1987; 11(11):953-959.
36. Spiro TE, Socquet M, Delforge A, Stryckmans P. Chemotherapeutic sensitivity of normal and leukemic hematopoietic progenitor cells to N-[4-(9-acridinylamino)-3-methoxyphenyl]-methanesulfonamide, a new anticancer agent. *J Natl Cancer Inst.* 1981;66(4):615-618.
37. Jiang B, Hattori N, Liu B, et al. Expression and roles of Cl- channel ClC-5 in cell cycles of myeloid cells. *Biochem Biophys Res Commun.* 2004;317(1):192-197.
38. Kunzelmann K. Ion channels and cancer. *J Membr Biol.* 2005;205(3):159-173.
39. Lang F, Foller M, Lang KS, et al. Ion channels in cell proliferation and apoptotic cell death. *J Membr Biol.* 2005;205(3):147-157.
40. Milton RH, Abeti R, Averaimo S, et al. CLIC1 function is required for beta-amyloid-induced generation of reactive oxygen species by microglia. *J Neurosci.* 2008;28(45):11488-11499.
41. Hussain S, Rodgers DA, Duhart HM, Ali SF. Mercuric chloride-induced reactive oxygen species and its effect on antioxidant enzymes in different regions of rat brain. *J Environ Sci Health B.* 1997;32(3):395-409.
42. Kotake-Nara E, Saida K. Endothelin-2/vasoactive intestinal contractor: regulation of expression via reactive oxygen species induced by CoCl2, and biological activities including neurite outgrowth in PC12 cells. *Sci World J.* 2006;6:176-186.
43. Kong Q, Beel JA, Lillehei KO. A threshold concept for cancer therapy. *Med Hypotheses.* 2000;55(1): 29-35.
44. Sawayama Y, Miyazaki Y, Ando K, et al. Expression of myeloperoxidase enhances the chemosensitivity of leukemia cells through the generation of reactive oxygen species and the nitration of protein. *Leukemia.* 2008;22(5):956-964.